Dyes and Pigments 96 (2013) 180–188

Contents lists available at SciVerse ScienceDirect

Dyes and Pigments

journal homepage: www.elsevier.com/locate/dyepig

Synthesis, spectral properties of cyanine dyes-β-cyclodextrin and their application as the supramolecular host with spectroscopic probe

Jun-Long Zhao, Ying Lv, Hai-Jing Ren, Wei Sun, Qi Liu, Yi-Le Fu, Lan-Ying Wang*

Key Laboratory of Synthetic and Natural Functional Molecule Chemistry, Ministry of Education, College of Chemistry and Materials Science, Northwest University, Xi'an 710069, PR China

ARTICLE INFO

Article history:
Received 11 November 2011
Received in revised form
6 August 2012
Accepted 6 August 2012
Available online 14 August 2012

Keywords:
Cyanine dye-β-cyclodextrin
Spectral properties
Supramolecular inclusion complex
Spectroscopic probe
1-Adamantanol
Vitamin B_6

ABSTRACT

Six new cyanine dye functionalised β-cyclodextrins were designed and synthesized to improve the drawback of the inadequate chromophore in β-cyclodextrin and to be suitable for the study of supramolecular interactions directly by visible spectroscopy. The dye structures were confirmed by ^{1}H NMR, IR, UV–Vis and HRMS. The UV–Vis spectra of the new cyanine dyes in different solvents were investigated. The inclusion behaviour of a quinocyanine derived β-cyclodextrin dye which was used as the supramolecular host with 1-adamantanol or vitamin B_6 was investigated. The results indicated that the stoichiometry for the inclusion complex of the quinocyanine derived β-cyclodextrin dye and both 1-adamantanol and vitamin B_6 was 1:1, and their inclusion constants were 9.39×10^4 L/mol and 6.14×10^2 L/mol, respectively. The quinocyanine derived β-cyclodextrin dye was also used as the supramolecular host for the analysis of vitamin B_6 in tablets with satisfactory results.

1. Introduction

Cyanine dyes present typical optical properties and act as one of the most important organic functional dyes [1,2]. These dyes have tunable wavelengths across the visible spectrum, and exhibit high molar extinction coefficients permitting the use of low concentrations [3]. β-cyclodextrin (β-CD), which has both hydrophobic cavity and hydrophilic surface, is considered as an attractive compound in the field of molecular recognition [4,5], enzyme mimics [6], construction of molecular building blocks with ordered nanostructures [7], commodity [8–11], medicine [12–14] and chemical industry [15–17]. However, β-CD shows poor molecular selectivity in molecular recognition. Therefore, chemically modified β-CD is studied extensively. β-CD was modified with quinoline to obtain the biquinolino-bridged bis-cyclodextrin, which included pyroninophilic dye at different pH to study the protonation and deprotonation of xanthene dyes [18]. Voncina et al. [19], grafted β-CD onto PET textile materials, which could be used as odour carriers or as malodorous absorbers. Suresh and Pitchumani [20], modified β-CD with amino to obtain per-6-amino-β-CD, acting simultaneously as a supramolecular ligand for CuI and host for aryl bromides, which could catalyse *N*-arylation of imidazole with aryl bromides under mild conditions. Yamada and Hashimoto [21], synthesized a water-soluble β-CD-immobilized poly (allylamine), then mixed the water-soluble β-CD derivatives and DNA to form inclusion complexes, which had the potential to absorb harmful compounds. However, there are no reports concerning the use of cyanine dye modified β-CDs as host compounds with spectroscopic probes to recognize colourless guest molecules [22,23].

In this study, six new cyanine dyes-β-CD were synthesized (Fig. 1) and characterized. Their UV–Vis spectra were investigated in different solvents. At the same time, the inclusion interaction of cyanine dye-β-CD (**6**) and 1-adamantanol (Fig. 2(a)) or vitamin B_6 (VB_6) (Fig. 2(b)) was studied by spectroscopic methods. Previously, the molecular recognition study on β-CD and its modified analogues with VB_6 was done using spectrophotometric titration by competitive inclusion method using guest molecules with chromophore or dyes as spectral probes [24,25]. In this work, synthetic dye-β-CD (**6**) had its own chromophore and could be used as a host compound with spectroscopic probe to recognize VB_6 without adding other spectral probes. This study describes the use of dyes-β-CD as host compounds with spectroscopic probes to recognize colourless guest molecules.

* Corresponding author. Tel.: +86 29 88302604; fax: +86 29 88303798.
E-mail address: wanglany@nwu.edu.cn (L.-Y. Wang).

0143-7208/$ – see front matter © 2012 Elsevier Ltd. All rights reserved.
http://dx.doi.org/10.1016/j.dyepig.2012.08.010

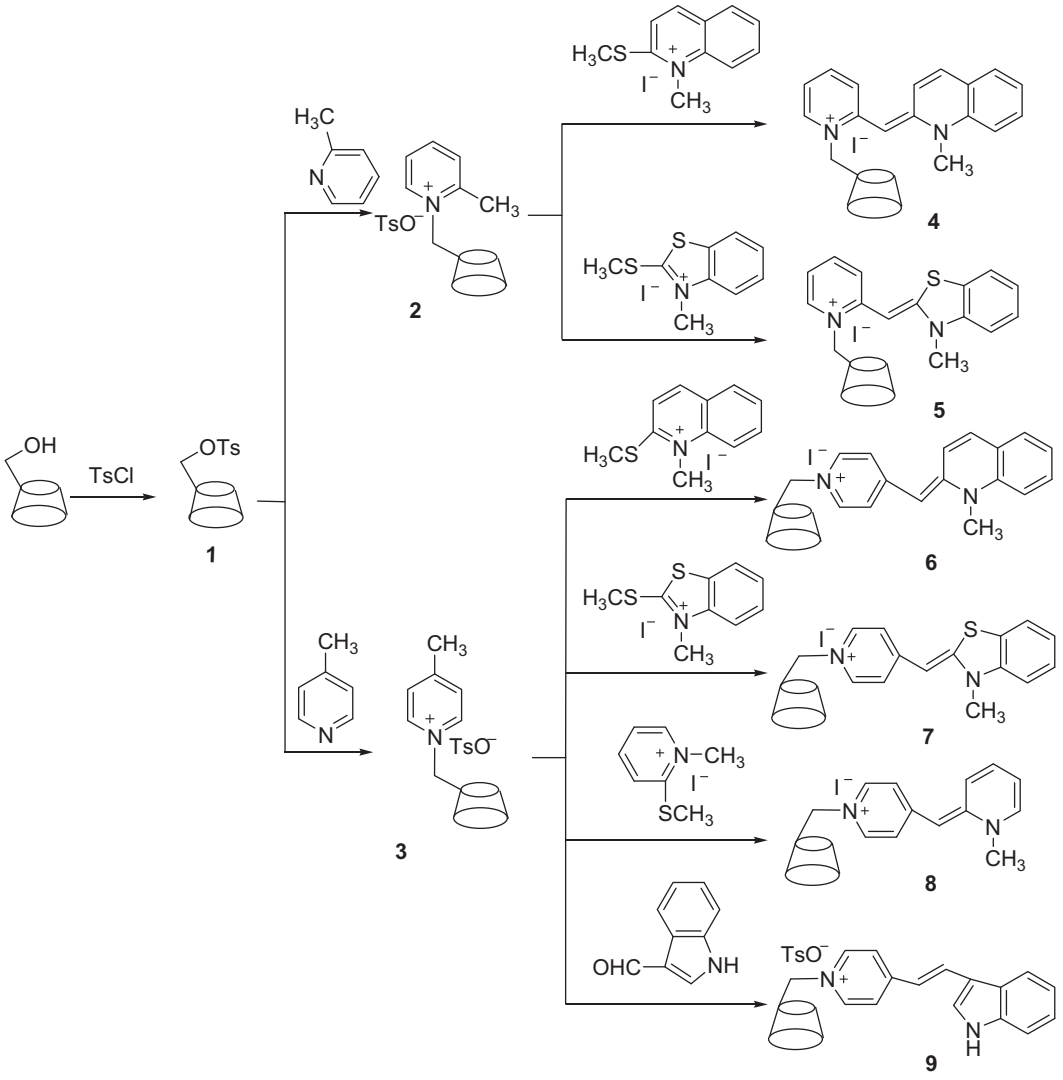

Fig. 1. Synthesis of dyes-β-CD.

2. Experimental

2.1. Chemicals and instruments

2.1.1. Chemicals

Commercially available reagents were used without additional purification. All solvents were of analytical grade.

2.1.2. Instruments

Melting points were taken on an XT-4 micromelting apparatus and uncorrected. IR spectra in cm^{-1} were recorded on a Bruker Equiox-55 spectrometer. The absorption spectra were recorded on a Purkinje General UV-1900 UV–Vis spectrometer. ^1H NMR spectra were recorded at 400 MHz on a Varian Inova-400 spectrometer and chemical shifts were reported relative to internal Me_4Si. HRMS was recorded on a microTOFQ II ESI-Q-ToF LC/MS/spectrometer.

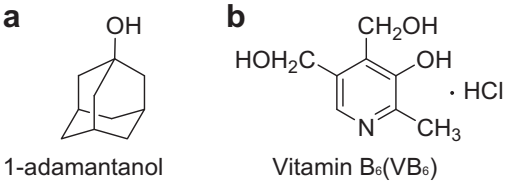

Fig. 2. Structures of 1-adamantanol (a) and VB_6 (b).

2.2. Synthesis of cyanine dyes-β-cyclodextrin

2.2.1. Mono-6-oxygen-tosyl-β-cyclodextrin (*1*)

Compound (**1**) was prepared according to the literature [26].

2.2.2. Mono-6-deoxy-6-(2-methylpyridinium)-β-cyclodextrin-p-toluenesulfonate (*2*)

Compound (**2**) was prepared according to the literature [27]. A mixture of compound (**1**) (2.70 g, 2.10 mmol) and 2-methyl pyridine (12.0 mL) was stirred at 85 °C for 12 h. After cooling, the solution was poured into acetone with stirring. The resulting precipitate was collected and purified with water and acetone (yield: 87%, m.p. 267–269 °C).

2.2.3. Mono-6-deoxy-6-(4-methylpyridinium)-β-cyclodextrin-p-toluenesulfonate (*3*)

Compound (**3**) was prepared according to the literature [27]. The same procedure described above but using 4-methyl pyridine (12.0 mL) (yield: 91%, m.p. 273–275 °C).

*2.2.4. Mono-6-deoxy-6-[2-(1-methyl-2-quinoline methyne) pyridinium]-β-cyclodextrin iodide (**4**)*

Compound (**2**) (1.37 g, 1.00 mmol) and 1-methyl-2-methylthioquinolinium iodide (0.31 g, 1.02 mmol) were dissolved in DMF (10.0 mL). Piperidine (0.8 mL) was added as a catalyst. The reaction mixtures were stirred at 75–80 °C for 5 h. After cooling to room temperature, the mixtures were poured into acetone under agitating, causing immediately formation of precipitate. The resulting precipitate was filtered off, dried and purified by silica gel chromatography (H_2O/EtOH/$NH_3 \cdot H_2O$, 6:2:2) and then recrystallised from H_2O:EtOH (2:1). Pure pink powder 0.25 g was obtained (yield: 17%), m.p.: >300 °C. UV–Vis (MeOH): λ_{max} = 472.0 nm (2.21×10^4 L mol^{-1} cm^{-1}). ^{1}H NMR (400 MHz, DMSO-d_6): δ = 2.72 (s, 3H, CH_3), 2.30–3.95 (m, 41H), 4.31–5.13 (m, 14H), 5.52–5.75 (m, 14H), 6.66 (s, 1H, CH=C), 7.18–7.51 (m, 6H, ArH), 7.91 (d, 2H, J = 7.6 Hz, pyridine), 8.63 (d, 2H, J = 7.6 Hz, pyridine) ppm. IR (KBr): υ = 3390 (s, υ_{-OH}), 2926 (s, υ_{C-H}), 1652, 1546, 1524 (m, $\upsilon_{C=C}$, $\upsilon_{C=N}$), 1466 (m, δ_{C-H}), 1155 (m, υ_{C-N}), 1029 (m, υ_{C-O-C}), 844 (m, $\delta_{=CH}$), 756 (m, $\delta_{=CH}$) cm^{-1}. HRMS (TOF MS ES-) calculated for $C_{58}H_{83}N_2O_{34}^+$: 1351.4822; found: 1351.4777.

*2.2.5. Mono-6-deoxy-6-[2-(3-methyl-2-benzothiazole methyne) pyridinium]-β-cyclodextrin iodide (**5**)*

The same procedure described above but using 3-methyl-2-methylthiobenzothiazolium iodide (0.33 g, 1.02 mmol) and stirring at 85–90 °C for 5 h gave crude product, which was purified by silica gel chromatography (H_2O/EtOH, 7:3) and then recrystallised from H_2O:EtOH (2:1). A yellow brown powder 0.17 g was obtained (yield: 11%), m.p.: >300 °C. UV–Vis (MeOH): λ_{max} = 450.0 nm (1.74×10^4 L mol^{-1} cm^{-1}). ^{1}H NMR (400 MHz, DMSO-d_6): δ = 2.78 (s, 3H, CH_3), 3.55–3.47 (m, 59H), 4.08–4.16 (m, 4H), 4.22–4.30 (m, 2H), 4.45–5.35 (m, 4H), 6.38(s, 1H, CH=C), 7.21–7.38 (m, 4H, PhH), 7.57 (d, 2H, J = 7.6 Hz, pyridine), 7.85 (d, 2H, J = 7.6 Hz, pyridine) ppm. IR (KBr): υ = 3420 (s, υ_{-OH}), 2924 (s, υ_{C-H}), 1655, 1600, 1502 (m, $\upsilon_{C=C}$, $\upsilon_{C=N}$), 1452 (m, δ_{C-H}), 1156 (m, υ_{C-N}), 1030 (m, υ_{C-O-C}), 845 (m, $\delta_{=CH}$), 785, 752 (m, $\delta_{=CH}$) cm^{-1}. HRMS (TOF MS ES-) calculated for $C_{56}H_{81}N_2O_{34}S^+$: 1357.4385; found: 1357.4352.

*2.2.6. Mono-6-deoxy-6-[4-(1-methyl-2-quinoline methyne) pyridinium]-β-cyclodextrin iodide (**6**)*

Compound (**3**) (1.37 g, 1.00 mmol) and 1-methyl-2-methylthioquinolinium iodide (0.31 g, 1.02 mmol) were dissolved in DMF (10.0 mL). Piperidine (0.8 mL) was added as a catalyst. The reaction mixtures were stirred at 75–80 °C for 3 h. After cooling to room temperature, the mixtures were poured into acetone under agitating, causing immediately formation of precipitate. The resulting precipitate was filtered off, dried and purified by silica gel chromatography (H_2O/EtOH/$NH_3 \cdot H_2O$, 6:2:2) and then recrystallised from H_2O:EtOH (2:1). Pure red powder 0.31 g was obtained (yield: 21%), m.p.: >300 °C. UV–Vis (MeOH): λ_{max} = 484.0 nm (2.63×10^4 L mol^{-1} cm^{-1}). ^{1}H NMR (400 MHz, DMSO-d_6): δ = 2.64 (s, 3H, CH_3), 2.30–3.95 (m, 41H), 4.10–5.30 (m, 14H), 5.01 (s, 1H, CH=C), 5.80–6.35 (m, 14H), 6.63–7.92 (m, 6H, ArH), 7.96 (d, 2H, J = 7.2 Hz, pyridine), 8.89 (d, 2H, J = 7.2 Hz, pyridine) ppm. IR (KBr): υ = 3442 (s, υ_{-OH}), 2926 (s, υ_{C-H}), 1640, 1567, 1524 (m, $\upsilon_{C=C}$, $\upsilon_{C=N}$), 1456, 1388 (m, δ_{C-H}), 1101 (m, υ_{C-N}), 1035 (m, υ_{C-O-C}), 885 (m, $\delta_{=CH}$), 786, 756 (m, $\delta_{=CH}$) cm^{-1}. HRMS (TOF MS ES-) calculated for $C_{58}H_{83}N_2O_{34}^+$: 1351.4822; found: 1351.4757.

*2.2.7. Mono-6-deoxy-6-[4-(3-methyl-2-benzothiazole methyne) pyridinium]-β-cyclodextrin iodide (**7**)*

The same procedure described above but using 3-methyl-2-methylthiobenzothiazolium iodide (0.33 g, 1.02 mmol) and stirring at 85–90 °C for 3 h gave crude product, which was purified by silica gel chromatography (H_2O/EtOH, 7:3) and then recrystallised from H_2O:EtOH (2:1). Pure yellow powder 0.28 g was obtained (yield: 19%), m.p.: >300 °C. UV–Vis (MeOH): λ_{max} = 452.0 nm (1.17×10^4 L mol^{-1} cm^{-1}). ^{1}H NMR (400 MHz, DMSO-d_6): δ = 2.29 (s, 3H, CH_3), 3.55–3.47 (m, 59H), 4.08–4.16 (m, 4H), 4.22–4.30 (m, 2H), 4.45–5.35 (m, 4H), 5.02–5.24 (m, 1H, CH=C), 5.91–6.10 (m, 2H, CH_2), 7.32–7.64 (m, 4H, PhH), 7.97 (d, 2H, J = 8.0 Hz, pyridine), 8.84 (d, 2H, J = 8.0 Hz, pyridine) ppm. IR (KBr): υ = 3385 (s, υ_{O-H}), 2928 (w, υ_{C-H}), 1641, 1522 (m, $\upsilon_{C=C}$, $\upsilon_{C=N}$), 1373 (m, δ_{C-H}), 1079, 1032 (s, υ_{C-O-C}), 945 (w, $\delta_{=CH}$) cm^{-1}. HRMS (TOF MS ES-) calculated for $C_{56}H_{81}N_2O_{34}S^+$: 1357.4385; found: 1357.4330.

*2.2.8. Mono-6-deoxy-6-[4-(1-methyl-2-pyridine methyne) pyridinium]-β-cyclodextrin iodide (**8**)*

The same procedure described above but using 1-methyl-2-methylthiopyridinium iodide (0.27 g, 1.02 mmol) and stirring at 70–80 °C for 3 h gave crude product, which was purified by silica gel chromatography (H_2O/EtOH/$NH_3 \cdot H_2O$, 7:2:1) and then recrystallised from H_2O:EtOH (2:1). Pure orange red powder 0.54 g was obtained (yield: 38%), m.p.: >300 °C. UV–Vis (MeOH): λ_{max} = 482.0 nm (1.07×10^4 L mol^{-1} cm^{-1}). ^{1}H NMR (400 MHz, D_2O): δ = 2.46 (s, 3H, CH_3), 3.40–3.96 (m, 69H), 6.64 (s, 1H, CH=C), 7.22–7.76 (m, 4H, pyridine), 8.16 (d, 2H, J = 7.4 Hz, pyridine), 8.80 (d, 2H, J = 7.4 Hz, pyridine) ppm. IR (KBr): υ = 3423 (s, υ_{-OH}), 2924 (s, υ_{C-H}), 1631, 1546, 1523, (m, $\upsilon_{C=C}$, $\upsilon_{C=N}$), 1476 (m, δ_{C-H}), 1157 (m, υ_{C-N}), 1030 (m, υ_{C-O-C}), 844 (m, $\delta_{=CH}$), 785, 755 (m, $\delta_{=CH}$) cm^{-1}. HRMS (TOF MS ES-) calculated for $C_{58}H_{81}N_2O_{34}^+$: 1301.4665; found: 1301.4599.

*2.2.9. Mono-6-deoxy-6-[4-(3-indole ethenyl) pyridinium]-β-cyclodextrin-p-toluenesulfonate (**9**)*

The same procedure described above but using 1H-indole-3-carboxaldehyde (0.15 g, 1.02 mmol) and stirring at 95–100 °C for 3 h gave crude product, which was purified by silica gel chromatography (H_2O/EtOH/$NH_3 \cdot H_2O$, 6:2:2) and then recrystallised from H_2O:EtOH (2:1). Pure yellow powder 0.24 g was obtained (yield: 16%), m.p.: >300 °C. UV–Vis (MeOH): λ_{max} = 444.0 nm (1.24×10^4 L mol^{-1} cm^{-1}). ^{1}H NMR (400 MHz, DMSO-d_6): δ = 3.55–3.47 (m, 59H), 4.08–4.16 (m, 4H), 4.22–4.30 (m, 2H), 4.45–5.35 (m, 4H), 5.61–6.02 (m, 4H, PhH), 7.17 (d, 2H, J = 16.2 Hz, CH=C), 7.51 (d, 2H, J = 7.8 Hz, pyridine), 8.67–8.74 (m, 3H, two phenyl and one vinylic protons), 9.21 (s, 1H, NH) ppm. IR (KBr): υ = 3423 (s, υ_{-OH}), 2924 (s, υ_{C-H}), 1656, 1526 (m, $\upsilon_{C=C}$, $\upsilon_{C=N}$), 1451 (m, δ_{C-H}), 1157 (m, υ_{C-N}), 1030 (m, υ_{C-O-C}), 855 (m, $\delta_{=CH)}$, 755 (m, $\delta_{=CH}$) cm^{-1}. HRMS (TOF MS ES-) calculated for $C_{57}H_{81}N_2O_{34}^+$: 1337.4665; found: 1337.4612.

2.3. Determination of absorption spectra of dyes-β-CD

The 1×10^{-4} M dyes-β-CD stock solutions were prepared by dissolving dyes-β-CD in DMSO and further diluted to the appropriate concentration with DMF, DMSO, water, ethanol and methanol, respectively. The absorption spectra were then recorded.

2.4. Determination of inclusion constant of the inclusion complex between dye-β-CD (**6**) and 1-adamantanol

In spectral measurements, NaH_2PO_4–Na_2HPO_4 buffer solution (0.1 M, pH = 7.2, methanol–water mixed solvents) was used as the solvent. The concentration of dye-β-CD (**6**) was kept constant, 1.82×10^{-5} M. The concentrations of 1-adamantanol were in the range from 0 M (a) to 8.99×10^{-3} M (i). The UV–Vis absorption spectra of these solutions were measured at 300.0–600.0 nm to evaluate the inclusion constant of the inclusion complex between dye-β-CD (**6**) and 1-adamantanol.

For a 1:1 stoichiometry, the inclusion complexation of guest 1-adamantanol (G) and host with spectroscopic probe dye-β-CD (**6**) (H) was expressed by Eq (1).

$$H + G = HG \quad (1)$$

Inclusion constant K_s could be expressed in the form of Eq. (2), where $[H]_0$ and $[G]_0$ were the initial concentrations of H and G; [H], [G] and [HG] were the equilibrium concentrations of H, G and HG, respectively.

$$K_s = \frac{[HG]}{[H] \times [G]} = \frac{[HG]}{([H]_0 - [HG]) \times ([G]_0 - [HG])} \quad (2)$$

In the experiment, if the concentrations of G and H were kept $[G]_0 \gg [H]_0$, the extended equation of Eq. (2) was shown below (Eq. (3)):

$$K_s = \frac{[HG]}{([H]_0 - [HG]) \times [G]_0} \quad (3)$$

Before the inclusion interaction of G and H, the absorbance properties of dye-β-CD were shown as follows (Eq. (4)) [28]:

$$A_0 = k_0[H]_0 \quad (4)$$

After coordination equilibrium was attained, the absorbance properties of dye-β-CD could be shown below (Eq. (5)):

$$A = k_0[H] + k_1[HG] = k_0([H]_0 - [HG]) + k_1[HG] \quad (5)$$

where k_0 and k_1 were defined as absorption coefficients. Eq. (4) was subtracted by Eq. (5), resulting in the following expression (Eq. (6)):

$$\Delta A = A_0 - A = (k_0 - k_1)[HG] = \Delta k[HG] \quad (6)$$

Eq. (6) was substituted into Eq. (3), then Benesi–Hildebrand Eq. (7) was obtained:

$$\frac{[H]_0}{\Delta A} = \frac{1}{K_s \times \Delta k \times [G]_0} + \frac{1}{\Delta k} \quad (7)$$

where Δk was sensitive coefficient of host's conformational changes during the process of inclusion. By plotting $[H]_0/\Delta A$ vs $1/[G]_0$, a linear relationship could be obtained. Inclusion constant K_s could be calculated from the intercept and slope.

2.5. Determination of inclusion constant of the inclusion complex between dye-β-CD (**6**) and VB_6

NaH_2PO_4–Na_2HPO_4 buffer solution (0.1 M, pH = 7.2, distilled water) was used as the solvent. The concentration of dye-β-CD (**6**) was kept constant, 2.70×10^{-5} M. The concentrations of VB_6 were in the range from 0 M (a) to 8.00×10^{-3} M (j). The UV–Vis absorption intensities of these solutions were measured at 300.0–600.0 nm to evaluate the inclusion constant of the inclusion complex between dye-β-CD (**6**) and VB_6.

2.6. Sample preparation

Forty pieces of VB_6 tablets (10 mg/piece) were crushed into a powder, and dissolved into distilled water. The sample was filtered and the filtrate was transferred into a 100 mL volumetric flask, and diluted to final volume with distilled water to afford stock solutions.

3. Results and discussion

3.1. Synthesis of cyanine dyes-β-CD

In all cases investigated, cyanine dyes-β-CD formation proceeded efficiently. The synthetic conditions of cyanine dyes-β-CD were listed in Table 1. From reaction temperature it could be found that the sequence of the reaction activity for mono-6-deoxy-6-(4-methylpyridinium)-β-cyclodextrin-*p*-toluenesulfonate (**3**) and various 2-methylthio heterocyclic quaternary salts or 1H-indole-3-carboxaldehyde was 1-methyl-2-methylthiopyridinium iodide ≈ 1-methyl-2-methylthioquinolinium iodide > 3-methyl-2-methy lthiobenzothiazolium iodide > 1H-indole-3-carboxaldehyde. This was because the conjugated degree of the dyes-β-CD formed by intermediate (**3**) and various 2-methylthio heterocyclic quaternary salts or 1H-indole-3-carboxaldehyde differed from each other. The larger the conjugated degree was, the more stable the formed dye-β-CD was, according to the Hammond postulate [29,30], the smaller the activation energy required for forming dye-β-CD was, and the faster the reactive rate was, that is, this reaction occurred more easily. The donor–π–acceptor (D–π–A) conjugated skeleton structures of dyes-β-CD (**6**), (**7**), (**8**) and (**9**) were showed respectively as follows:

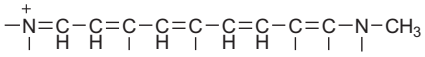

(6) or (8)

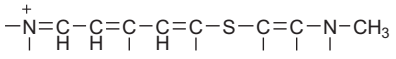

(7)

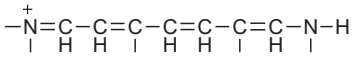

(9)

Table 1
The synthetic conditions of cyanine dyes-β-CD.

Dyes-β-CD	Reactant		Reaction temperature (°C)	Reaction time (h)
4	2	1-methyl-2-methylthioquinolinium iodide	75–80	5
5		3-methyl-2-methylthiobenzothiazolium iodide	85–90	5
6	3	1-methyl-2-methylthioquinolinium iodide	75–80	3
7		3-methyl-2-methylthiobenzothiazolium iodide	85–90	3
8		1-methyl-2-methylthiopyridinium iodide	70–80	3
9		1H-indole-3-carboxaldehyde	95–100	3

In the conjugated structure, when the group –S– was bonded to the D–π–A framework, there was p–π conjugation, and when a –CH=CH– unit was bonded to the D–π–A framework, there was π–π conjugation, and the conjugated degree of π–π was greater than that of p–π. In addition, when the electron-donating group was NMe, the methyl group exhibited σ–p hyperconjugation effect through its sigma orbit and p orbit of N, thus an NMe could be considered to be a better donor group than an NH. Therefore the size of the conjugated degree of dyes-β-CD (**6**), (**7**), (**8**) and (**9**) was (**6**) ≈ (**8**) > (**7**) > (**9**), and the sequence of the reaction activity was 1-methyl-2-methylthiopyridinium iodide ≈ 1-methyl-2-methylthioquinolinium iodide > 3-methyl-2-methylthiobenzothiazolium iodide > 1H-indole-3-carboxaldehyde.

The synthetic cyanine dyes-β-CD were not easily purified, because of their high molecular weight, the presence of several hydroxyl groups and their association with either small reactant molecules or solvent molecules. In this paper, the end products were initially purified according to their differing solubility in various solvents. The preliminary purification was effected by precipitation from acetone followed silica gel chromatography.

3.2. UV–Vis absorption spectra properties of cyanine dyes-β-CD

The absorption spectra of dyes-β-CD (**6**), (**7**) and (**8**) in different solvents were shown in Fig. 3. It could be seen that the influence of solvents on the absorption spectra of dye-β-CD (**7**) was different from that of dyes-β-CD (**6**) and (**8**). This phenomenon was attributed to the fact that the D–π–A structures of these three dyes-β-CD were different. In dyes-β-CD (**6**), (**7**) and (**8**), their electron acceptor was the same, while the electron donor was different. In dye-β-CD (**7**) the electron donor was a benzothiazole nucleus, but in dyes-β-CD (**6**) and (**8**) the electron donor was a quinoline and a pyridine nucleus, respectively, and quinoline and pyridine nucleus had similar structure and properties. The absorbance properties of dyes-β-CD (**4**)–(**9**) in different solvents were summarized in Table 2. It could be found that the maximum absorption wavelengths (λ_{max}) of the same dye-β-CD showed variations in different solvents. The λ_{max} of the same dye-β-CD in aprotic solvent was DMSO > DMF, but the λ_{max} in the protic solvent showed no such order. The experimental results also revealed that the sequence of the λ_{max} was (**6**) ≈ (**8**) > (**4**) > (**7**) > (**5**) > (**9**) in the same solvent. The reason was that the λ_{max} was related to the size of the conjugated system of dyes-β-CD. The greater the conjugated system of dyes-β-CD was, the greater the λ_{max} was. Based on the previous analysis, the size of the conjugated system of dyes-β-CD (**4**)–(**9**) was (**6**) ≈ (**8**) > (**4**) > (**7**) > (**5**) > (**9**), leading to the λ_{max} of dyes-β-CD was (**6**) ≈ (**8**) > (**4**) > (**7**) > (**5**) > (**9**) in the same solvent.

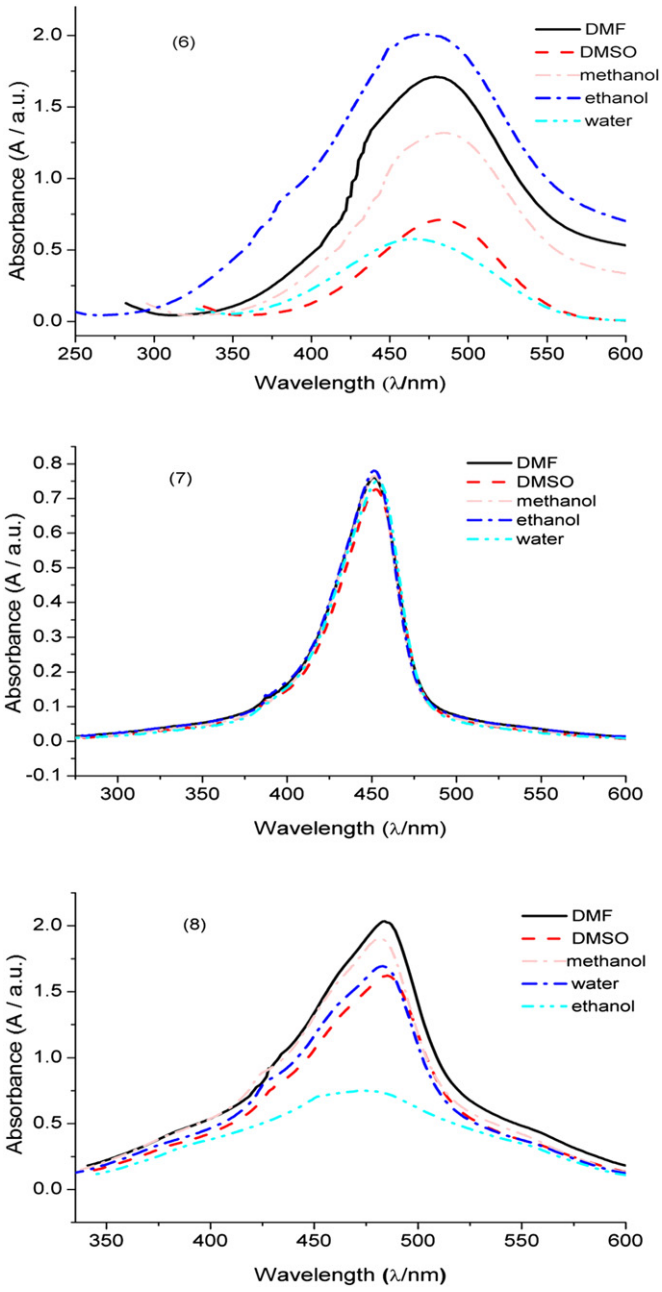

Fig. 3. Absorption spectra of dyes-β-CD (**6**), (**7**) and (**8**) in different solvents.

3.3. The self-inclusion interactions of dye-β-CD (6) molecules

Structural model of control dye, control β-CD, dye-β-CD (**6**) and the self-inclusion interactions of dye-β-CD (**6**) molecules for each other were represented in Fig. 4. The chemical shifts of partial protons in control dye, control β-CD and dye-β-CD (**6**) in D_2O solvent were summarized in Tables 3 and 4.

From Table 3, we could see that: (i) Chemical shifts of H(c), H(d), H(e), H(f), H(g), H(h) and H(CH_3) in dye-β-CD (**6**) shifted to high field compared with the control dye. These shifts indicated that the quinoline ring entered into the cavity of the β-CD in dye-β-CD (**6**) [31]. (ii) The upfield shift was obvious in H(f), H(g), H(h) and H(CH_3), but relatively less in H(c), H(d) and H(e); this feature indicated that the quinoline ring entered into the cavity of β-CD in the equator direction, but did not enter vertically into the cavity of β-CD (Fig. 4). H(f), H(g), H(h) and H(CH_3) were close to the inner wall of β-CD, so they were affected by protons in the cavity of β-CD.

From Table 4 it could be seen that: (i) H(3) and H(5) in dye-β-CD (**6**) absorbed at higher field compared with the control β-CD. It further demonstrated that quinoline ring entered into the cavity of β-CD at equator direction, and effected on H(3) and H(5) in dye-β-CD (**6**) molecules, which led to the chemical shifts of H(3) and H(5) in dye-β-CD (6) shifting to higher field. (ii) Chemical shift of H(5) in dye-β-CD (**6**) changed significantly, which suggested that the quinoline ring entered deeply into the cavity of β-CD, making H(5) in dye-β-CD (**6**) absorb at higher field. Besides, the carbon chain between D–π–A system and β-CD in dye-β-CD (**6**) molecules was short and it was thus impossible for the quinoline ring in dye-β-CD (**6**) to enter into its own cavity. In other words, dye-β-CD (**6**) had intermolecular inclusion interaction, and the quinoline ring of one dye-β-CD (**6**) molecule entered into the cavity of another dye-β-CD (**6**) molecule.

Table 2
Physical properties of solvent, the λ_{max} and ε of dyes-β-CD in different solvents.

Dyes-β-CD	Solvent	MeOH	H_2O	EtOH	DMF	DMSO
	Dielectric constant	32.63	78.39	24.55	37.60	48.90
4	λ_{max}/nm	472.0	463.0	461.0	467.0	470.0
	$\varepsilon \times 10^{-4}$/L mol^{-1} cm^{-1}	2.21	1.75	3.96	3.11	1.79
5	λ_{max}/nm	450.0	449.0	448.0	448.0	450.0
	$\varepsilon \times 10^{-4}$/L mol^{-1} cm^{-1}	1.74	1.52	1.81	2.51	2.15
6	λ_{max}/nm	484.0	464.0	470.0	479.0	483.0
	$\varepsilon \times 10^{-4}$/L mol^{-1} cm^{-1}	2.63	1.15	4.02	3.42	1.42
7	λ_{max}/nm	452.0	453.0	451.0	451.0	452.0
	$\varepsilon \times 10^{-4}$/L mol^{-1} cm^{-1}	1.17	1.15	1.12	1.16	1.11
8	λ_{max}/nm	482.0	483.0	475.0	484.0	485.0
	$\varepsilon \times 10^{-4}$/L mol^{-1} cm^{-1}	1.07	0.95	0.42	1.15	0.91
9	λ_{max}/nm	444.0	433.0	449.0	434.0	441.0
	$\varepsilon \times 10^{-4}$/L mol^{-1} cm^{-1}	1.24	0.92	1.25	1.44	1.06

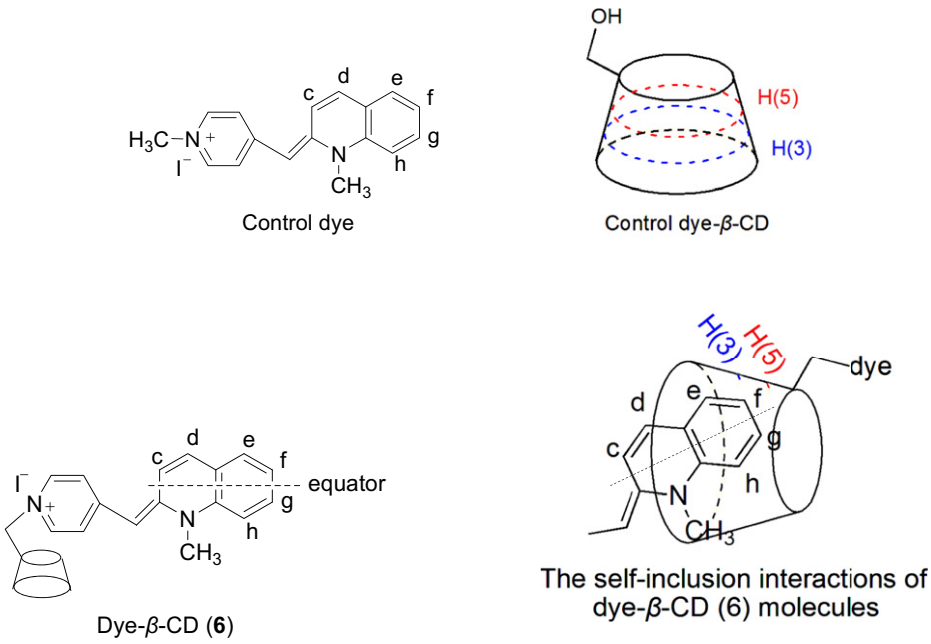

Fig. 4. Structural model of control dye, control β-CD, dye-β-CD (**6**) and the self-inclusion interactions of dye-β-CD (**6**) molecules.

*3.4. Inclusion complexation stoichiometry of dye-β-CD (**6**) with 1-adamantanol*

In order to determine the stoichiometry for the formation of the inclusion complex of dye-β-CD (**6**) with 1-adamantanol, the continuous variation method was used. In NaH_2PO_4–Na_2HPO_4 buffer solutions (0.1 M, pH = 7.2, methanol–water mixed solvents), the total concentration of dye-β-CD (**6**) and 1-adamantanol was kept constant, 2.0×10^{-5} M, and the ratio of the two components was changed continuously. The absorbance difference (ΔA) between dye-β-CD (**6**) and miscible liquids of dye-β-CD (**6**) and 1-adamantanol was measured under the same condition, and the stoichiometry could be obtained by plotting ΔA vs mole fraction of any component. A Job's plot for the complexation of dye-β-CD (**6**) with 1-adamamtanol was shown in Fig. 5(a). According to the range of dye-β-CD (**6**), the plot showed a maximum at the molar fraction of 0.5, which indicated the formation of 1:1 inclusion complex.

*3.5. The inclusion interactions of dye-β-CD (**6**) and 1-adamantanol*

The absorption spectra of dye-β-CD (**6**) in the presence of 1-adamantanol were shown in Fig. 6. It could be seen that the λ_{max} of dye-β-CD (**6**) was not changed with the addition of 1-adamantanol, and the absorption intensity of dye-β-CD (**6**) was regularly increased with the increasing concentrations of 1-adamantanol. The reason was that the chromophoric group of one dye-β-CD (**6**) molecule entered into the hydrophobic cavity of another dye-β-CD (**6**) molecule in the solution of dye-β-CD (**6**). When 1-adamantanol was added into the solution, the

Table 3
Chemical shifts of protons in control dye and dye-β-CD (**6**) in D_2O solvent.

	H(c)	H(d)	H(e)	H(f)	H(g)	H(h)	H(CH_3)
Control dye	7.57	7.54	7.59	7.31	7.50	7.61	3.69
Dye-β-CD (**6**)	7.56	7.53	7.53	7.18	7.19	7.51	2.86
$\Delta\delta$	0.01	0.01	0.06	0.13	0.31	0.10	0.83

Table 4
Chemical shifts of H(3) and H(5) in control β-CD and dye-β-CD (**6**) in D_2O solvent.

	H(3)	H(5)
Control β-CD	3.96	3.84
Dye-β-CD (**6**)	3.78	3.49
$\Delta\delta$	0.18	0.35

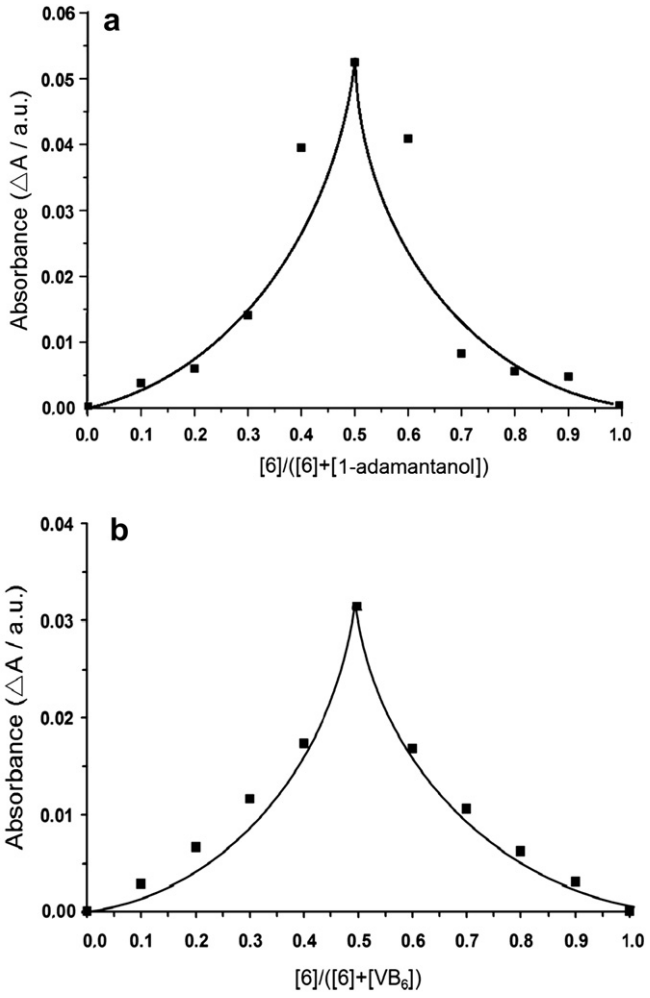

Fig. 5. Job's plot of the complexation of dye-β-CD (**6**) with 1-adamantanol or VB_6 in buffer solution. (a) [**6**] + [1-adamantanol] = 2.00×10^{-5} M; (b) [**6**] + [VB6] = 4.00×10^{-5} M.

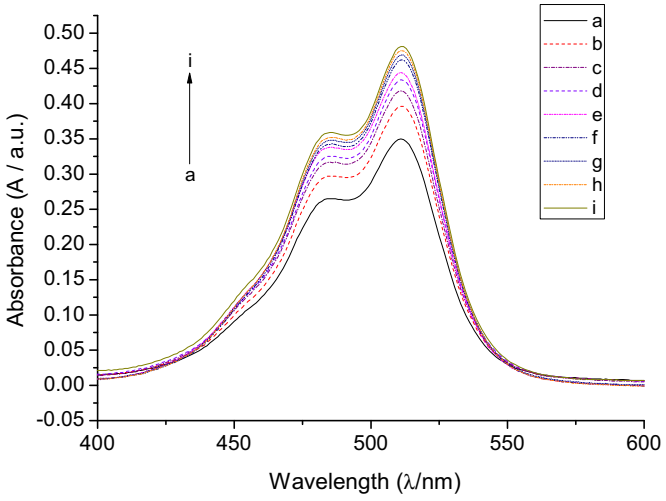

Fig. 6. UV–Vis spectra of dye-β-CD (**6**) (1.82×10^{-5} M) in the presence of 1-adamantanol in NaH_2PO_4–Na_2HPO_4 buffer solution (pH = 7.2). The concentrations of 1-adamantanol: (a) 0 M; (b) 1.97×10^{-3} M; (c) 2.97×10^{-3} M; (d) 3.99×10^{-3} M; (e) 5.03×10^{-3} M; (f) 6.00×10^{-3} M; (g) 7.00×10^{-3} M; (h) 8.01×10^{-3} M; (i) 8.99×10^{-3} M.

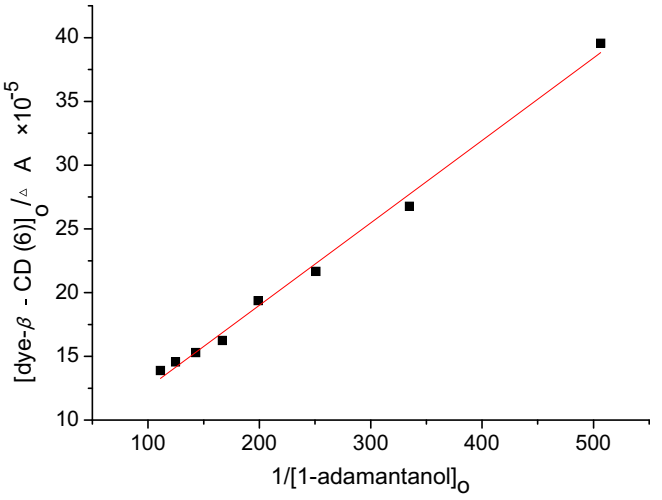

Fig. 7. Benesi–Hildebrand analyses for the inclusion complexation of dye-β-CD (**6**) with 1-adamantanol.

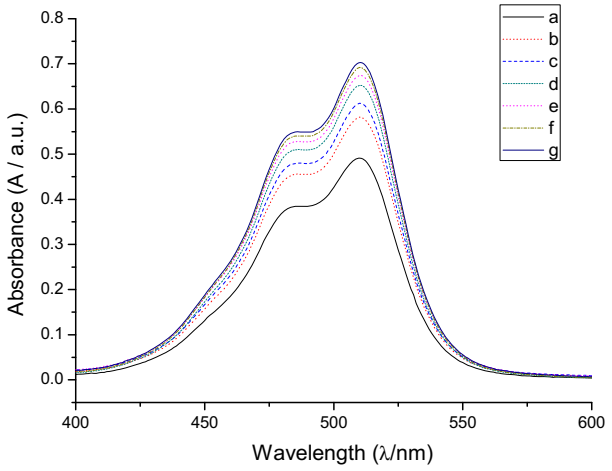

Fig. 8. UV–Vis spectra of dye-β-CD (**6**) (2.70×10^{-5} M) in the presence of VB_6 in NaH_2PO_4–Na_2HPO_4 buffer solution (pH = 7.2). The concentrations of VB_6: (a) 0 M; (b) 1.00×10^{-3} M; (c) 2.00×10^{-3} M; (d) 4.50×10^{-3} M; (e) 6.00×10^{-3} M; (f) 7.00×10^{-3} M; (g) 8.00×10^{-3} M.

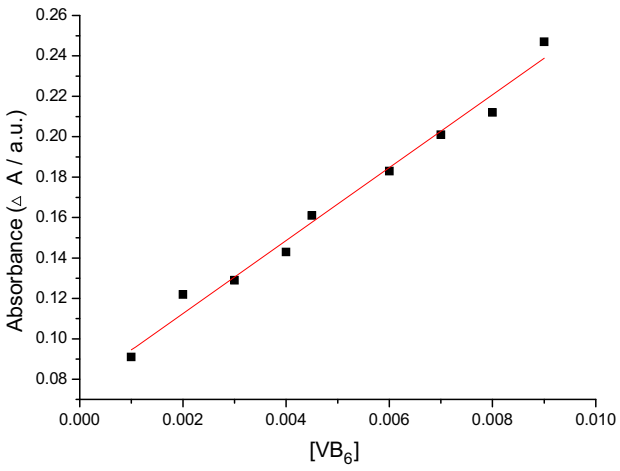

Fig. 9. Linear relationship between the concentrations of VB_6 (1.00×10^{-3}–9.00×10^{-3} M) and the absorbance changes (ΔA) in the system of VB_6 and dye-β-CD (**6**) (2.70×10^{-5} M).

Table 5
The results of determination of the samples ($n = 6$).

The absorbance of the samples (A)	The absorbance changes of the systems (ΔA)	The measured concentration (mol/L)	The calculated content (mg/piece)	Relative error (%)	RSD (%)
0.614	0.124	2.63×10^{-3}	9.67	−3.3	0.83
0.620	0.130	2.97×10^{-3}	9.59	−4.1	
0.634	0.144	3.74×10^{-3}	9.62	−3.8	
0.645	0.155	4.35×10^{-3}	9.73	−2.7	
0.652	0.162	4.74×10^{-3}	9.81	−1.9	
0.662	0.172	5.29×10^{-3}	9.72	−2.8	

chromophoric group of dye-β-CD (**6**) was not replaced out of the cavity by 1-adamantanol, on the contrary, the 1-adamantanol induced the geometric complement between the chromophoric group and the cavity of β-CD [32,33]. Namely, the chromophoric group was included deeper than in absence of 1-adamantanol. Thus, the absorption intensities increased regularly.

The Benesi–Hildebrand analyses about the inclusion complexation of dye-β-CD (**6**) with 1-adamantanol were shown in Fig. 7. Our data gave $y = 0.0647x + 6.0746$ ($R = 0.9972$), and according to this formula, the inclusion constant of dye-β-CD (**6**) and 1-adamantanol was determined to be 9.39×10^4 L/mol. The result corresponded to the conclusion mentioned above, that is, the ratio of dye-β-CD (**6**) to 1-adamantanol was 1:1.

3.6. Inclusion complexation stoichiometry of dye-β-CD (6) with VB_6

In order to determine the stoichiometry for the formation of the inclusion complex of dye-β-CD (**6**) with VB_6, the continuous variation method was used. In NaH_2PO_4–Na_2HPO_4 buffer solutions (0.1 M, pH = 7.2, with distilled water as solvent), the total concentration of dye-β-CD (**6**) and VB_6 was kept constant, 4.0×10^{-5} M, and the ratio of the two components was changed continuously. The absorbance difference (ΔA) between dye-β-CD (**6**) and miscible liquids of dye-β-CD (**6**) and VB_6 was measured under the same condition. The stoichiometry could be obtained by plotting ΔA vs mole fraction of any component. A Job's plot for the complexation of dye-β-CD (**6**) with VB_6 was shown in Fig. 5(b). According to the range of dye-β-CD (**6**), the plot showed a maximum at the mole fraction of 0.5, which indicated the formation of 1:1 inclusion complex.

3.7. The inclusion interactions of dye-β-CD (6) and VB_6

Absorption spectra of dye-β-CD (**6**) in the presence of VB_6 were located at the same spectral region as the corresponding free dye-β-CD (**6**). The absorption intensity of dye-β-CD (**6**) was regularly increased with an increase of VB_6 concentration (Fig. 8). For a 1:1 stoichiometry, according to the extended Benesi–Hildebrand equation (Eq. (7)), a linear relationship could be obtained ($y = 1.8707 \times 10^{-7}x + 1.1495 \times 10^{-4}$, $R = 0.9902$). The result again proved the ratio of dye-β-CD (**6**) to VB_6 was 1:1. The inclusion constant was 6.14×10^2 L/mol.

3.8. Sample analysis

The synthetic dye-β-CD (**6**) was used as the spectroscopic probe to analyse VB_6 content in tablets, on the basis of the linear relationship between the concentration of VB_6 and the absorbance changes (ΔA) in the system of VB_6 and dye-β-CD (**6**). VB_6 content in tablets was determined with the linear relationship ($y = 18.0388x + 0.0765$, $R = 0.9923$) (Fig. 9). The analytical results were shown in Table 5. It could be seen that the content of VB_6 in tablets was determined to be 9.69 ± 0.12 mg/piece (Marked content 10.00 mg/piece) and the relative standard deviation (RSD) was 0.83% ($n = 6$). Compared with detection methods reported in the literature, this method was simple and fast, and could obtain satisfactory results.

4. Conclusions

Six new cyanine dyes-β-CD were designed and synthesized. The synthetic cyanine dyes-β-CD displayed good absorption properties. The inclusion interactions of dye-β-CD (**6**) as the supramolecular host with 1-adamantanol or VB_6 showed that dye-β-CD (**6**) could form a (1:1) inclusion complex with either 1-adamantanol or VB_6, with the inclusion constants of 9.39×10^4 L/mol and 6.14×10^2 L/mol, respectively. What is more, dye-β-CD (**6**) could be applied to the spectroscopic analysis of VB_6 in tablets with satisfactory results.

Acknowledgement

We appreciate the financial support for this research by a grant from the Scientific and Technological Research and Development Projects in Shaanxi Province (2012K07-06), the Special Science Research Foundation of Education Committee (No. 11JK0558).

References

[1] Shindy HA, El-Maghraby MA, Eissa FM. Synthesis and colour spectrophotometric measurements of some novel merocyanine dyes. Dyes Pigm 2012; 92(2):929–35.
[2] Fürstenberg A, Julliard MD, Deligeorgiev TG, Gadjev NI, Vasilev AA, Vauthey E. Ultrafast excited-state dynamics of DNA fluorescent intercalators: new insight into the fluorescence enhancement mechanism. J Am Chem Soc 2006; 128(23):7661–9.
[3] Bricks J, Ryabitskii A, Kachkovskii A. Studies of 2-azaazulenium derivatives: the natures of electron transitions in the 2-azaazulenium cation and in monomethine cyanine dyes bearing 2-azaazulenium moieties as terminal groups. Eur J Org Chem 2009;2009(20):3439–49.
[4] Sun HY, Bai Y, Zhao MG, Hao AY, Xu GY, Shen J, et al. New cyclodextrin derivative 6-O-(2-hydroxybutyl)-β-cyclodextrin: preparation and its application in molecular binding and recognition. Carbohydr Res 2009;344(15): 1999–2004.
[5] Surpateanu GG, Becuwe M, Lungu NC, Dron PI, Fourmentin S, Landy D, et al. Photochemical behaviour upon the inclusion for some volatile organic compounds in new fluorescent indolizine β-cyclodextrin sensors. J Photochem Photobiol A 2007;185(2–3):312–20.
[6] Fu H, Zhou YH, Chen WL, Deqing ZG, Tong ML, Ji LN, et al. Complexation, structure, and superoxide dismutase activity of the imidazolate-bridged dinuclear copper moiety with β-cyclodextrin and its guanidinium-containing derivative. J Am Chem Soc 2006;128(15):4924–5.
[7] Fan Z, Guo MJ, Diao CH, Jing ZL, Chen X, Wang M. The structure of interlocked helical supramolecule formed by the self-assembly of mono-6-(4-cyanophenyl)-β-cyclodextrin. Solid State Sci 2010;12(5):834–8.
[8] Yang Y, Yang HF, Liu YL, Liu ZM, Shen GL, Yu RQ. Cetyltrimethylammonium assay using fluorescence probe berberine and a competitive host-guest complexation with butylated β-cyclodextrin. Sens Actuators B 2005;106(2): 632–40.
[9] Esmaeili MA, Yazdanparast R. Beta-cyclodextrin-bonded silica assists alkaline phosphatase and carbonic anhydrase refolding in a solid phase assisted refolding approach. Process Biochem 2010;45(2):239–46.
[10] He HB, Zhang WN, Da SL, Feng YQ. Preparation and characterization of a magnesia-zirconia stationary phase modified with β-cyclodextrin for reversed-phase high-performance liquid chromatography. Anal Chim Acta 2004;513(2):481–92.

[11] Ju JF, Syu MJ, Teng HS, Chou SK, Chang YS. Preparation and identification of β-cyclodextrin polymer thin film for quartz crystal microbalance sensing of benzene, toluene, and p-xylene. Sens Actuators B 2008;132(1):319–26.
[12] Bencini M, Ranucci E, Ferruti P, Trotta F, Donalisio M, Cornaglia M, et al. Preparation and in vitro evaluation of the antiviral activity of the acyclovir complex of a β-cyclodextrin/poly(amidoamine) copolymer. J Control Release 2008;126(1):17–25.
[13] Meng H, Xue M, Xia T, Zhao YL, Tamanoi F, Stoddart JF, et al. Autonomous in vitro anticancer drug release from mesoporous silica nanoparticles by pH-sensitive nanovalves. J Am Chem Soc 2010;132(36):12690–7.
[14] Yano H, Kleinebudde P. Improvement of dissolution behavior for poorly water-soluble drug by application of cyclodextrin in extrusion process: comparison between melt extrusion and wet extrusion. AAPS PharmSciTech 2010;11(2):885–93.
[15] Skold ME, Thyne GD, Drexler JW, McCray JE. Solubility enhancement of seven metal contaminants using carboxymethyl-β-cyclodextrin. J Contam Hydrol 2009;107(3–4):108–13.
[16] Yilmaz A, Yilmaz E, Yilmaz M, Bartsch RA. Removal of azo dyes from aqueous solutions using calyx[4]arene and β-cyclodextrin. Dyes Pigm 2007;74(1):54–9.
[17] Hussain LA, Dickens SH, Bowen RL. Effects of polymerization initiator complexation in methacrylated β-cyclodextrin formulations. Dent Mater 2004;20(6):513–21.
[18] Song Y, Chen Y, Liu Y. Switchable fluorescence behaviors of pyronine Y at different pH values upon complexation with biquinolino-bridged bis(β-cyclodextrin). J Photochem Photobiol A 2005;173(3):328–33.
[19] Voncina B, Vivod V, Chen WT. Surface modification of PET fibers with the use of β-cyclodextrin. J Appl Polym Sci 2009;113(6):3891–5.
[20] Suresh P, Pitchumani K. Per-6-amino-β-cyclodextrin as an efficient supramolecular ligand and host for Cu(I)-catalyzed N-arylation of imidazole with aryl bromide. J Org Chem 2008;73(22):9121–4.
[21] Yamada M, Hashimoto K. DNA–cyclodextrin composite material for environmental applications. Biomacromolecules 2008;9(12):3341–5.
[22] Ren HJ, Wang LY, Zhang XH, Wang YX, Zhang ZX. Synthesis of a hemicyanine dye-β-cyclodextrin and its inclusion with 1-adamantanol. Sci J NWU Online 2010;8(3):0233 [2010-05-10].
[23] Huang YD, Yu HT, Wang YM, Meng JB. Synthesis and properties of β-cyclodextrin bearing a spiro [2H-benzopyran-2,2′-indoline] moiety. Chem J Chin U 2001;22(10):1685–7.
[24] Zhu XS, Sun J, Wu J. Study on the inclusion interactions of β-cyclodextrin and its derivative with dyes by spectrofluorimetry and its analytical application. Talanta 2007;72(1):237–42.
[25] Liu XP, Yang Y, Zhang GM, Dong C, Shuang SM. Study on the inclusion interaction of vitamin B_6 and β-cyclodextrin and its derivatives by competitive fluorescence inclusion method. Fenxi Huaxue 2003;31(8):996–9.
[26] Petter RC, Salek JS, Sikorski CT, Kumaravel G, Lin FT. Cooperative binding by aggregated mono-6-(alkylamino)-β-cyclodextrins. J Am Chem Soc 1990;112(10):3860–8.
[27] Wang LY, Li FM, Huang Y, Mei MY, Zhang ZX. Synthesis and properties of novel hemicyanine dyes-β-cyclodextrin. Chin J Chem 2007;25(08):1192–5.
[28] Wang R, Yu ZW. Validity and reliability of Benesi–Hildebrand method. Acta Phys Chim Sin 2007;23(9):1353–9.
[29] Michael BS, March J. March's advanced organic chemistry—reactinons, mechanisms, and structure. Translated by Li YM. 5th ed. Beijing: Chemical Industry Press; 2009.
[30] Kang Q, Fan FL, Bi WB, Huang Y, Fu YL, Wang LY. Microwave-assisted synthesis and spectral properties of some benzoindohemicyanine and benzoindodimethine cyanine dyes as well as the interaction with biomolecules. Chin J Org Chem 2012;32(3):567–73.
[31] Tang YL, Feng J, Xiang JF, Chen CP, Yan WP, Xu GZ. Study of the dynamic structures and equilibria of β-cyclodextrin with cyanine dyes. Chin J Magn Reson 2001;18(2):161–7.
[32] Liu Y, Zhang YM, Qi AD, Wang QC, Chen RD. Molecular recognition study on supramolecular system. Chin Sci Bull 1998;43(2):166–8.
[33] Ikeda H, Murayama T, Ueno A. Skeleton-selective fluorescent chemosensor based on cyclodextrin bearing a 4-amino-7-nitrobenz-2-oxa-1,3-diazole moiety. Org Biomol Chem 2005;3(23):4262–7.